Strain relief through stair-rod dislocations in ultrathin epitaxial metal films: Defect geometry and energetics

A. Klein, W. Meyer, A. Schmidt, B. Gumler, S. Müller, L. Hammer, and K. Heinz
Lehrstuhl für Festkörperphysik, Universität Erlangen-Nürnberg, Staudtstr. 7, D-91058 Erlangen, Germany
(Received 14 May 2008; published 21 July 2008)

Epitaxial Ni films deposited on Ir(100) were investigated by tunneling microscopy (STM), quantitative low-energy electron diffraction (LEED), and density-functional theory (DFT). For film thicknesses beyond 3 monolayers the large tensile strain (≈9%) is relieved by the formation of stair-rod-like dislocations. Their favorable energetics is revealed by DFT calculations which also determine the defects' structural parameters. On the unstructured Ir(100)−(1×1) surface they develop in an irregular way, i.e., without long-range order. In STM they are visible as shallow depressions or by decoration with further adsorbed adatoms. In contrast to this case of missing long-range order, the dislocations are ordered in films on the Ir(100)−(5×1)-H surface, whereby (5×1)-periodic Ir wires at the interface act as pinning centers. So, their detailed atomic structure is accessible experimentally by quantitative LEED with crystallographic precision. Features similar to Ni are also observed for Co films.

DOI: 10.1103/PhysRevB.78.045422 PACS number(s): 61.72.Dd, 61.72.Ff, 68.35.−p, 68.55.−a

I. FOCUS

As well known, ultrathin heteroepitaxial films resulting by pseudomorphic growth on a crystalline substrate can be substantially strained according to the epitaxial misfit between the substrate and the native film material. Usually, starting at a certain film thickness so-called misfit dislocations develop reducing the stress accompanied by the strain within the film. The large majority of the corresponding investigations are for surfaces with hexagonally close-packed atomic layers, as fcc(111) and hcp(0001) for elemental metals. The stress relief comes by domains with laterally different stackings at the interface; i.e., there are laterally alternating domains with fcc and hcp sites occupied whereby, depending on the substrate, one of the domains represents a stacking fault. The shift between the two differently stacked domains (Burgers vector) is no full lattice vector; i.e., the distortion corresponds to Shockley partial dislocations with the dislocation core between the surface and second layer. In the transition region between the hcp and fcc domains, the film atoms reside in intermediate sites of reduced coordination symmetry (compared to hcp and fcc sites). Thereby the lateral atomic spacing is reduced or increased, so reducing tensile or compressive stress, respectively. A corresponding system investigated in much detail is, for example, Cu/Ru(0001) (see, e.g., Refs. 1 and 2).

For epitaxial films on fcc(001) surfaces no stacking faults in surface parallel layers are possible. Yet, it has been found in early work on the epitaxial system Ni/Cu(001) that strain relief can come by misfit dislocations with Burgers vectors inclined by 45° with respect to the film plane.[3] For the reverse system, Cu/Ni(001), in which pseudomorphic Cu layers are under compressive stress, the strain relief was reported to be realized by so-called internal (111) faceting[4] whereby stacking faults in buried {111} planes within the film (inclined to each other) are formed. While the pseudomorphic strain is −2.5%, it relaxes to below −1% at about 20 monolayers (ML) coverage. A similar kind of misfit accommodation was found for the epitaxial growth of KCl on NaCl(100).[5]

In the present paper we report on a strain relief mechanism for the epitaxial systems Ni/Ir(100) and Co/Ir(100) which for pseudomorphic growth are—different from the case of Cu/Ni(100) mentioned above—under heavy *tensile* strain ($\epsilon_{Ni}=8.9\%$, $\epsilon_{Co}=8.3\%$). For the Ir(100)−(1×1) substrate we will show by scanning tunneling microscopy (STM) and quantitative low-energy electron diffraction (LEED) combined with first-principles calculations applying density-functional theory (DFT) that strain relief is achieved by the formation and interaction of two Shockley partial dislocations at different {111} glide planes, equivalent to stacking faults there. They meet and react with each other at or near the (100) interface where they form a defect similar to *Lomer-Cotrell* dislocation in the bulk of a material where the whole scenario is also known as stair-rod dislocation. Similar stress-induced defects have been found earlier both in experimental work and theoretical simulations (e.g., Refs. 6–12). In the present work we provide both the energetics and detailed geometry of the defect by DFT calculations. Moreover we show that, while the defects develop in an irregular way in films on the Ir(100)−(1×1) substrate, they form an almost regular array when the metal is deposited on the phase Ir(100)−(5×1)-H. Induced by hydrogen this surface is reconstructed exhibiting a periodic arrangement of iridium wires of single atomic width which pin the dislocations. This makes the latter accessible to quantitative LEED so that we get the structural details of the defects for this case from experiment.

II. EXPERIMENTAL AND COMPUTATIONAL DETAILS

The experiments were performed using a two-stage ultrahigh-vacuum (UHV) apparatus hosting a homemade four-grid LEED optics and a commercial beetle-type STM with easy transfer between the two parts.[13] STM images were taken at room temperature; the tip voltages and tunneling currents for the different images are given in the corresponding figure captions. LEED patterns and intensity vs energy spectra, $I(E)$, were recorded for normal incidence of the

primary electron beam and the sample at liquid air temperature. Thereby a 12 bit digital charge-coupled-device camera viewing the LEED screen from outside the UHV is used with the video signal evaluated under computer control.[14]

The Ir(100) substrate was prepared as two different phases by chemical treatment of the stable and reconstructed quasihexagonal surface Ir(100)$-(5\times1)$-hex.[15] Adsorption of oxygen followed by thermal activation and chemical reduction of the oxygen by exposure to hydrogen produces a clean and well ordered bulklike terminated surface, Ir(100)$-(1\times1)$.[16–18] It is metastable when clean but stabilized by adsorbates. Exposure of the (5×1)-hex phase to hydrogen above about 190 K also causes the surface to restructure whereby, however, the (5×1) periodicity is maintained. The 20% atoms additionally accommodated in the hexagonal surface layer are expelled to form a new surface layer in which they arrange as linear and close-packed chains of single atomic width in fivefold lateral periodicity.[19,20] This Ir(100)$-(5\times1)$-H structure is stabilized by hydrogen which, however, can be replaced by other species, in particular, metallic adsorbates.[21] For metal deposition an electron-beam evaporator supplied with the highly purified metal was used operated at a deposition rate of about 0.5 ML/min (1 ML corresponds to a coverage of 1.36×10^{15} cm^{-2}). The sample was either kept at about 370 K during deposition or annealed at that temperature after deposition leading to equal results.

By metal deposition on Ir(100)$-(1\times1)$ the symmetry of the LEED pattern stays to be (1×1), only the intensity spectra change. Equivalently, the (5×1) symmetry of the pattern remains with deposition on Ir(100)$-(5\times1)$-H, again only the intensities are modified. The $I(E)$ spectra were structurally analyzed by application of the perturbation method TensorLEED (Refs. 14, 22, and 23) using the ERLANGEN code.[24] A frustrated simulated annealing procedure[25] was applied for the structural search which was controlled by the Pendry R factor.[26] Besides the geometrical parameters also the layer-dependent atomic thermal vibration amplitudes were varied within the search as well as the occupation of lattice sites near the interface by different atomic species in order to check for intermixing.

In order to check for the stability of different configurations of the various epitaxial films and to determine their structure from first principles we applied DFT for Ni and Co films of different thicknesses. The Vienna ab-initio simulation package (VASP) (Ref. 27) was used with the projector augmented wave[28,29] method. For the exchange-correlation functional the general gradient approximation[30] was applied. The epitaxial system was described by asymmetric slabs consisting of the number of deposited metal layers and six iridium layers below them with three of the latter kept fixed to simulate the bulk of the substrate. For the structural search for deviations off the ideal (1×1) atomic arrangement in the layers a lateral supercell of (9×1) size proved to be sufficient.

III. INSTABILITY OF IDEALLY PSEUDOMORPHIC FILMS

Deposition of up to 3 ML Ni on Ir(100)$-(1\times1)$ leads to pseudomorphic growth resulting in rather flat films as illustrated in Fig. 1(a) for a Ni coverage of slightly above 3 ML with small square islands already nucleated in the fourth layer. After completion of the latter there is a change in growth morphology: The fifth layer starts with the formation of narrow chains with all of the same width as demonstrated in Fig. 1(b). Further deposition first leads to an increased number of irregularly arranged chains which more and more coalesce to compact islands. Eventually, a closed layer is formed on which, upon further metal deposition, chains reappear, again without long-range order as demonstrated in Fig. 1(c) for the fifth layer almost completed and the sixth one starting to grow by chains. In Fig. 1(d) the image for an intermediate coverage is displayed. It demonstrates that layer growth is realized by the growth of the chains' length and, additionally, by nucleation and growth of islands between the chains. At 6 ML the layer-by-layer growth starts to gradually turn toward the Stranski-Krastanov which is demonstrated by Fig. 1(f). Zooming into a completed layer reveals that—even though the surface appears flat on a large scale—there are height variations within the surface with areas sunk in by up to 0.4 Å, as demonstrated in Figs. 2(a) and 2(b) for the sixth layer. Even in case of the third layer [Figs. 2(c) and 2(d)], on which "normal" growth is observed, such corrugated regions can be found, however, only in close vicinity of a surface defect [as indicated in Fig. 2(c) by an arrow] which seems to stabilize them.

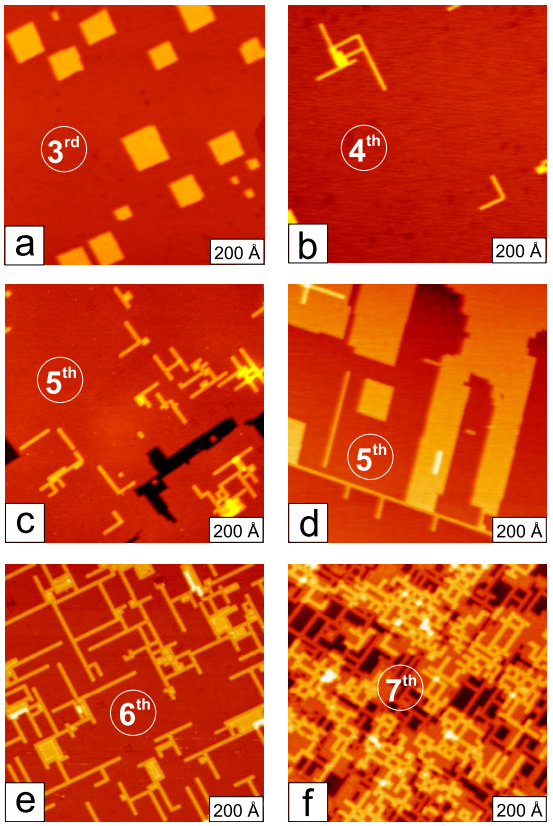

FIG. 1. (Color online) STM images for Ni films at about (a) 3 ML ($U=-261$ mV, $I=570$ pA), (b) 4 ML ($U=-500$ mV, $I=472$ pA), (c) 5 ML ($U=-199$ mV, $I=3{,}06$ nA), (d) 5.5 ML ($U=273$ mV, $I=477$ pA), (e) 6 ML ($U=500$ mV, $I=1.87$ nA), and (f) 7 ML ($U=3$ mV, $I=3.33$ nA).

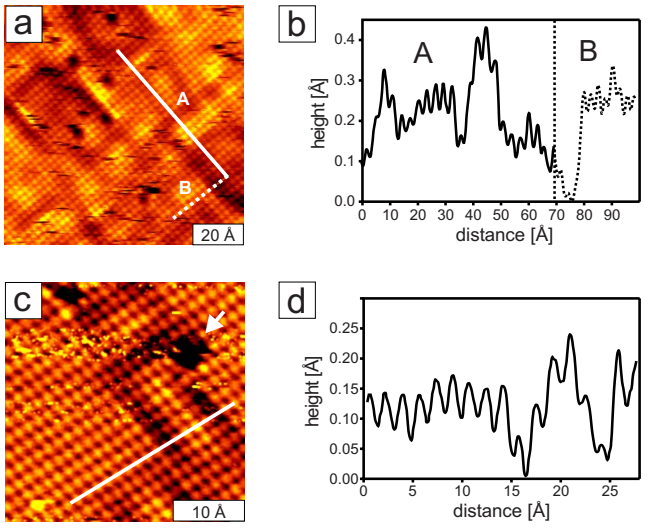

FIG. 2. (Color online) [(a) and (c)] STM images and [(b) and (d)] profiles [along the lines inserted in (a) and (c)] for [(a) and (b)] 6 ML and [(c) and (d)] 3 ML Ni film. In (a) depressions form already a kind of network while in (c) a depression is found near a surface defect indicated by an arrow. The STM parameters are (a) 51 mV, I=4.9 nA and (c) U=−3 mV, I=4.4 nA and (b).

The analyses of LEED intensities for Ni/Ir(100)−(1 × 1) surfaces with a completed layer and assuming that all layers are ideally pseudomorphic and flat yield excellent comparisons of experimental and model intensities quantified by Pendry R factors[26] as low as R=0.1 or even below (we do not give the resulting structural parameters as the assumption of flat films is wrong). Yet, this excellent fit quality is only possible by allowing for vibrational atomic amplitudes in all layers up to a factor of two above the bulk value (e.g., 0.140 Å in the top layer compared to 0.073 Å as bulk value for the square root of the mean-square amplitude). This is much above the frequently observed increase by a factor of $\sqrt{2}$ beyond the bulk value as due to surface bond truncation. It is indicative for positional (static) disorder within the surface according to common experience in quantitative LEED. This interpretation is in agreement with the above mentioned height variations within the surface.

As a consequence of the appearance of the depressions epitaxial films as flat and ideally pseudomorphic layer arrangements should be unstable. To check for that by DFT calculations an initial perturbation by a small positional shift to a surface atom was applied to the flat surface layer. We find that around this perturbation the film transforms to a wedgelike structure as displayed in Fig. 3 for a Ni film of 4 ML thickness on Ir(100)−(1 × 1). Evidently, within the wedge and in its surroundings there are lateral and vertical atomic shifts of up to about 0.4 Å. The overall restructuring of the film is in a way that the wedgelike structure appears to be sunk into the surface. The corresponding depth for the 4 ML Ni film as taken from the parameters displayed in Fig. 3 amounts to 0.4–0.5 Å. DFT calculations for a 5 ML film result in rather similar parameters. The calculated height variation is in agreement with the height difference retrieved from STM [Fig. 2(d)].

As shown in Table I the energetically favorable restructuring starts at 4 ML Ni. Yet, at 3 ML the energy cost is

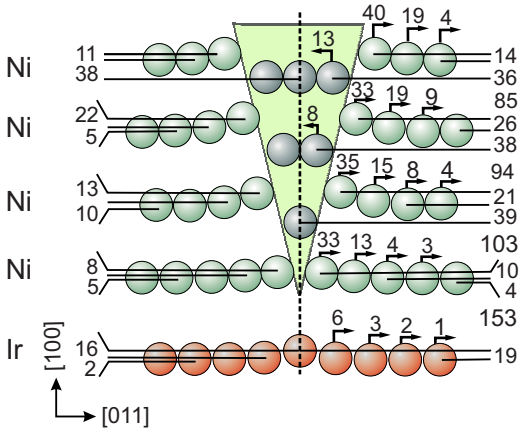

FIG. 3. (Color online) Ball model (side view) with structural parameters (given in pm) as determined by DFT calculations for the wedgelike defect in a 4 ML Ni film (note that only every second row of atoms is in the same plane and the vertical spacings and displacements are largely exaggerated). The lateral shifts refer to displacements off the ideally pseudomorphic positions. The mirror plane assumed is indicated by the broken line.

rather small so that a defect within the film seems to be sufficient to pin or stabilize a wedge which otherwise would only fluctuate at room temperature [Fig. 2(b)]. It is by decoration of those troughs formed by the wedges that the chainlike structures as displayed in Figs. 1(b)–1(d) appear. With further metal deposition the chains grow in length and additional islands nucleate and grow between them until the layer is completed. Then, however, new troughs develop due to the instability of the completed layer which are again decorated when the next layer starts to grow, etc.

We have also carried out equivalent DFT calculations for Co films. As shown in Table I the energy gain is considerably larger than for Ni films and starts already at 2 ML Co. The wedgelike structural scenario is very similar to that calculated for Ni, only the quantities of the different model parameters (given in Fig. 3 for Ni) vary slightly. The appearance of decorated wedges for 2 ML Co and higher is also confirmed by STM images. Yet, we here concentrate on Ni films as the further investigations presented below were carried only for them.

IV. FORMATION OF PERIODIC DEFECTS AND THEIR STRUCTURAL ANALYSIS

Up to this point, experimental support for the defects described came only by the increased positional disorder de-

TABLE I. Energetics of the wedge formation within Ni and Co films of different thicknesses d. The energies are relative to the defect-free ideally pseudomorphic films and refer to a (9 × 1) unit mesh of the slab calculated.

d (ML)	2	3	4	5
ΔE(Ni) (meV)		+17	−92	−316
ΔE(Co) (meV)	−63	−118	−411	−761

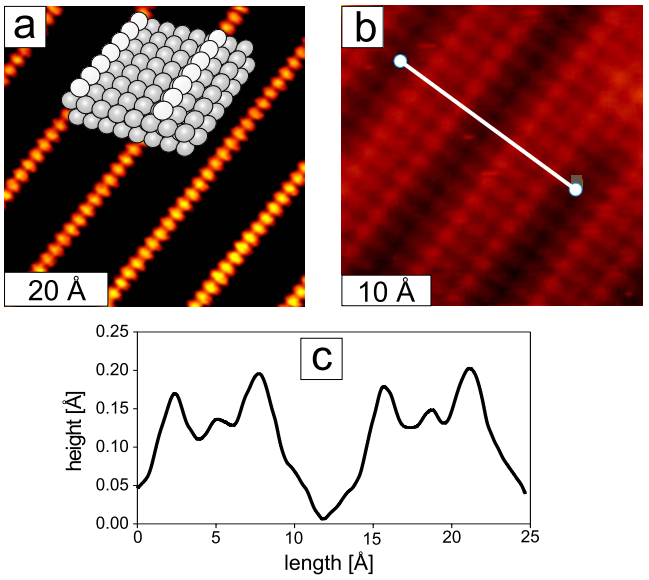

FIG. 4. (Color online) (a) STM image of the uncovered Ir(100)−(1×5)-H phase with the model retrieved by LEED inserted (after Ref. 19). (b) STM image of a 3.8 ML Ni film $U=-2.75$ mV, $I=4.99$ nA. Panel (c) displays the profile along the line inserted in panel (b).

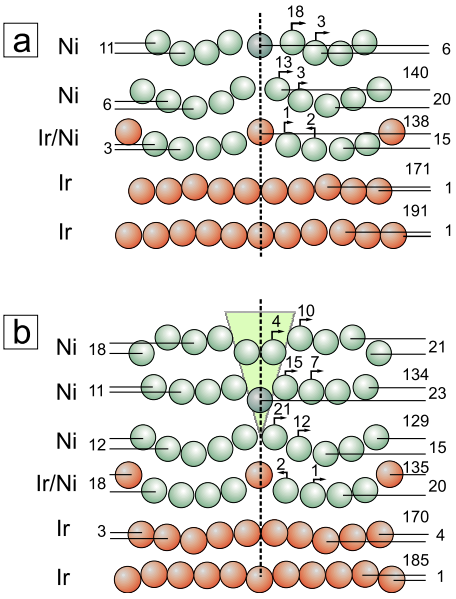

FIG. 5. (Color online) (a) Ball models (side view) and structural parameters (in pm units) retrieved by LEED for the (a) 2.8 ML and (b) 3.8 ML Ni film on Ir(100)−(1×5)-H. The lateral atomic shifts are with respect to the positions in flat ideally pseudomorphic layers.

tected by quantitative LEED analyses and by the different height areas appearing in STM. Quantitative LEED to resolve the wedge-type structure predicted by DFT is not applicable because of missing long-range order of the defects. Yet, we have found a way to produce an almost regular array of such defects by depositing the metal on Ir(100)−(5×1)-H instead of Ir(100)−(1×1). An STM image of the (5×1)-H phase with a ball model inserted is shown in Fig. 4(a). Only the Ir chains (which appear in fivefold periodicity on average) show up in the image. After deposition of about 3.8 ML Ni on that phase (note that completion of the substrate's top layer needs only 0.8 ML), the STM image displayed in Fig. 4(b) results. Clearly, there are again different height levels which now are, however, in an almost periodic arrangement according to that of the iridium chains at the interface. The STM profile displayed in Fig. 4(c) shows that the height variation is of the order of 0.2 Å if electronic effects can be neglected.

In order to follow the development of wedges we have structurally analyzed the LEED intensities for a 2.8 ML and a 3.8 ML Ni film. In both cases we achieve a convincing quality for the fit of model intensities to the experimental data (Pendry R factors of 0.14 and 0.13, respectively). We find no intermixing of the adatoms with substrate atoms. The structural results are displayed in panels (a) and (b) of Fig. 5. Clearly, the 2.8 ML film is just like an adsorption system with the adlayers residing carpetlike on the substrate (with some modifications of atomic positions in the substrate). At 3.8 ML coverage, however, wedges start to develop: As obvious from comparison of panels (a) and (b) of Fig. 5 the center Ni atom (dark shaded) above the interface Ir atom sinks into the surface when going from 2.8 to 3.8 ML coverage. This is the nucleus of a wedge which forms by the Ni neighbors above that nucleus in the next layer(s). They also sink into the surface as shown in Fig. 5(b) for the top layer. Error limits estimated by the variance of the Pendry R factor[26] are of the order of 0.01–0.02 Å for layer spacings and bucklings in the top two layers and 0.02–0.03 Å for surface parallel shifts and bucklings in deeper layers as investigated in detail for the (5×1)-hex phase which is of similar structural complexity.[15]

V. DISCUSSION AND CONCLUSION

As shown in the preceding paragraphs ideally pseudomorphic Ni (and Co) films on the flat Ir(100)−(1×1) substrate are unstable and reconstruct locally. The wedgelike structures predicted by DFT (Fig. 3) and observed by STM (Fig. 2) are characterized by—besides vertical atomic displacements—additional and rather large surface parallel atomic shifts which are of the order of 0.3–0.4 Å. The whole wedge is somewhat sunk into the surface so that it appears as a depression in STM when stabilized by a surface defect or as a thin chain of adatoms when these decorate the wedge. The defects allow the tensile strain of the pseudomorphic layers to relieve to some extent as, locally, atoms can move closer to each other. In fact, stress measurements for Ni/Ir(100)−(1×1) prove that a 15 GPa stress in a pseudomorphic film is drastically reduced beyond 2 ML Ni.[31] The onset of this stress relief process by defect formation is invisible in the LEED pattern since the average lateral spacing of atoms remains the same. On the (5×1) periodically structured Ir(100)−(5×1)-H substrate ideally pseudomorphic epitaxial films are also unstable so that wedge-shaped defects for stress relief develop, too. Yet, here they are pinned by the interface structure, i.e., the Ir wires at the interface. This is in

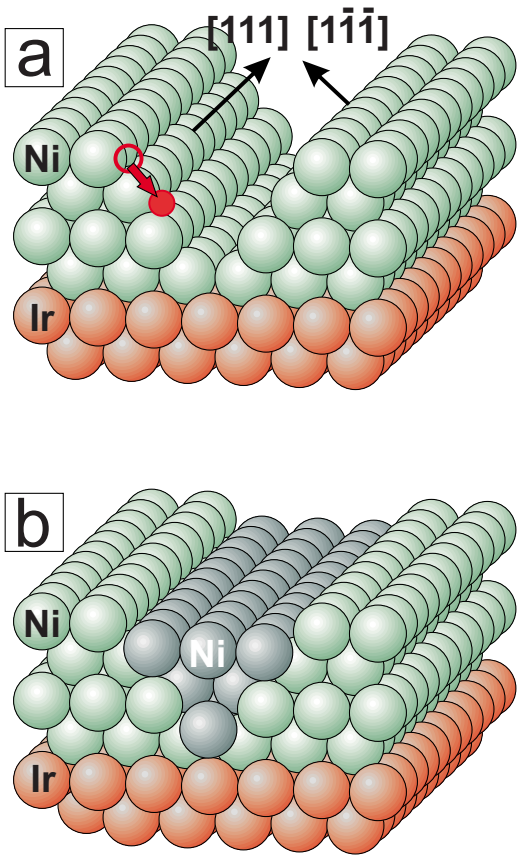

FIG. 6. (Color online) Schematic appearance of the wedgelike defect in a 4 ML Ni film. In panel (a) the film is shown with the atoms forming the wedge removed. A fcc (hcp) site is indicated by an open (filled) circle with the Burgers vector between them given by the (red) arrow. Panel (b) displays the sunk-in wedge after formation of the stair-rod dislocation.

line with our speculation that it needs a defect to stabilize a wedge locally in very thin films.

The principal mechanism of the restructuring of the flat and strained films can be understood as the interaction of two partial dislocations taking place at the (111) and (1$\bar{1}\bar{1}$) faces bordering the wedge as displayed in Fig. 6 with the wedge omitted. An fcc site is indicated by an open circle in one of the {111} surfaces in panel (a). The down-hill neighbored hcp site is also indicated (filled circle) and the related Burgers vector $\vec{b}_1=\frac{a}{6}[\bar{2}11]$ describing the partial dislocation taking place is inserted as an arrow ($\vec{b}_2=\frac{a}{6}[\bar{2}\bar{1}\bar{1}]$ holds for the Burgers vector on the opposite (1$\bar{1}\bar{1}$) face). All atoms at the wedge's edge plane undergo a partial dislocation (according to the Burgers vector). The result of the interaction of the two dislocations, which meet at their apex and eventually form a stair-rod dislocation, is displayed in Fig. 6(b). The sunk-in wedge—with the sinking-in mainly due to the down-hill movements of the atoms on the {111} faces—is apparent. Of course, the sinking-in is only possible by simultaneous lateral displacements of the atoms surrounding the wedge. These lateral displacements as experimentally determined by LEED for the (5×1)-periodic arrangement [Fig. 5(b)] are smaller (though being still substantial) than calculated by DFT for a dislocation in a (9×1) unit cell. Obviously, due to the enforced experimental periodicity there is less room for lateral relaxations than calculated. This might also be the reason that the amount by which the wedges are sunk into the surface is considerably smaller than the value corresponding to the full Burgers vector. Therefore, we tend to denote the defects as stair-rod-like dislocations. The DFT result, according to which the energy gain in Co films is higher than in Ni films, can be understood by the fact that partial dislocations in fcc Co films cost less energy than in Ni films as hcp and fcc stacking is almost energetically degenerate in Co in contrast to Ni.

In the literature, work on thin fcc(100) films under tensile strain is rare, in particular, with respect to information about the energetics and crystallography. Yet, similar defects as in the present work have been found to be created by nanoindentations of a Au(100) surface.[6] In this small-scale hardness test a STM tip punches perfect dislocation loops into the surface consisting of *V*-shaped half-loops which intersect the surface with the Burgers vector parallel to the latter. They split into Shockley partials held up by a stair-rod dislocation parallel to the surface. This gives rise to the formation of hillocks at the surface, rather than sunk-in structures as in our case. This is probably due to the fact that nanoindentations produce compressive stress rather than tensile stress we have in the present investigation. Wedgelike structures have also been found for epitaxial semiconductor systems, e.g., compressively strained InGaAs/GaAs(100) (Ref. 7) with aggregation of vancancies—which diffuse in from the surface—suspected to play an important role in the formation of the defects. A few theoretical papers deal also with cases of tensile stress. So, simulations of hydrostatic tension exerted on bulk Al found that nanovoids are formed from which, with increasing strain, dislocations are emitted.[9] For unidirectional tension (⟨100⟩ direction) in Ni the interaction of Shockley partials and stair rods was investigated by atomistic simulations.[8] For a four-layered model Ni/Cu/Ni/Cu (with three interfaces involved and $\epsilon=2.6\%$) calculations applying the embedded atom method found the formation of stair-rod dislocations at the interface by rebounding glide dislocations.[10] Molecular-dynamics simulations of the deposition of Ni nanoclusters on Cu(100) found stair rods locked at the interface after Shockley partial dislocations on different slip planes have met there.[11] Yet, this formation sensitively depends on the layer thickness and energy of the Ni cluster arriving at the Cu surface. So, in parallel investigations[12] formation of the defects was observed for clusters of at least 8 ML thickness. This compares qualitatively with our case of Ni/Ir(100) for which—at a considerably higher tensile strain—stair-rod-like defects are observed only for films of at least 4 ML thickness.

In conclusion we have shown that Ni or Co films deposited on Ir(100), which would be under heavy tensile stress when arranged in pseudomorphic configuration, are unstable from the second (Co) or third (Ni) layer on. Stress relief comes by the formation of stair-rod-like dislocations which appear at the surface as sunk-in atomic wedges. With further deposition these dislocations are decorated in the first place so that the growth of the next layer starts by chain like structures. This procedure is repeated after completion of each

layer until, beyond about 6 ML for Ni, Stranski-Krastanov growth starts. While the dislocations are irregularly distributed on the isotropic Ir(100)(1×1) surface they exhibit long-range order when the metal is deposited on the laterally structured Ir(100)$-(5\times1)$ phase. It turns out that they preferably form above this substrate's linear, atomically narrow, and laterally periodically arranged Ir wires which appear to act as pinning centers. The periodic arrangement of the defects allows us to access the structure of this stair-rod-like dislocations also experimentally with crystallographic precision.

ACKNOWLEDGMENTS

The authors are indebted to Deutsche Forschungsgemeinschaft (DFG) for financial support.

[1] C. Günther, J. Vrijmoeth, R. Q. Hwang, and R. J. Behm, Phys. Rev. Lett. **74**, 754 (1995).
[2] F. El Gabaly, W. L. W. Ling, K. F. McCarty, and J. de la Figuera, Science **308**, 1303 (2005).
[3] J. W. Matthews and J. L. Crawford, Thin Solid Films **5**, 187 (1970).
[4] B. Müller, B. Fischer, L. Nedelmann, A. Fricke, and K. Kern, Phys. Rev. Lett. **76**, 2358 (1996).
[5] M. Henzler, C. Homann, U. Malaske, and J. Wollschläger, Phys. Rev. B **52**, R17060 (1995).
[6] O. Rodríguez de la Fuente, J. A. Zimmerman, M. A. González, J. de la Figuera, J. C. Hamilton, W. W. Pai, and J. M. Rojo, Phys. Rev. Lett. **88**, 036101 (2002).
[7] A. G. Cullis, A. J. Pidduck, and M. T. Emeny, Phys. Rev. Lett. **75**, 2368 (1995).
[8] M. I. Baskes, R. G. Hoagland, and T. Tsuji, Modell. Simul. Mater. Sci. Eng. **6**, 9 (1998).
[9] J. Marian, J. Knap, and M. Ortiz, Phys. Rev. Lett. **93**, 165503 (2004).
[10] C. H. Henager and R. G. Hoagland, Scr. Mater. **50**, 701 (2004).
[11] J. C. Jiménez-Sáez, A. M. C. Pérez-Martín, M. Said-Ettaoussi, and J. J. Jiménez-Rodríguez, Nanotechnology **16**, 396 (2005).
[12] J. C. Jiménez-Sáez, A. M. C. Pérez-Martín, M. Said-Ettaoussi, and J. J. Jiménez-Rodríguez, Nucl. Instrum. Methods Phys. Res. B **228**, 64 (2005).
[13] C. Giovanardi, L. Hammer, and K. Heinz, Phys. Rev. B **74**, 125429 (2006).
[14] K. Heinz, Rep. Prog. Phys. **58**, 637 (1995).
[15] A. Schmidt, W. Meier, L. Hammer, and K. Heinz, J. Phys.: Condens. Matter **14**, 12353 (2002).
[16] J. Küppers and H. Michel, Appl. Surf. Sci. **3**, 179 (1979).
[17] K. Heinz, G. Schmidt, L. Hammer, and K. Müller, Phys. Rev. B **32**, 6214 (1985).
[18] D. Lerch, A. Klein, A. Schmidt, S. Müller, L. Hammer, K. Heinz, and M. Weinert, Phys. Rev. B **73**, 075430 (2006).
[19] L. Hammer, W. Meier, A. Klein, P. Landfried, A. Schmidt, and K. Heinz, Phys. Rev. Lett. **91**, 156101 (2003).
[20] K. Heinz and L. Hammer, J. Phys. Chem. B **108**, 14579 (2004).
[21] A. Klein, A. Schmidt, L. Hammer, and K. Heinz, Europhys. Lett. **65**, 830 (2004).
[22] P. J. Rous, J. B. Pendry, D. K. Saldin, K. Heinz, K. Müller, and N. Bickel, Phys. Rev. Lett. **57**, 2951 (1986).
[23] P. J. Rous and J. B. Pendry, Prog. Surf. Sci. **39**, 3 (1992).
[24] V. Blum and K. Heinz, Comput. Phys. Commun. **134**, 392 (2001).
[25] M. Kottcke and K. Heinz, Surf. Sci. **376**, 352 (1997).
[26] J. B. Pendry, J. Phys. C **13**, 937 (1980).
[27] G. Kresse and J. Furthmüller, Phys. Rev. B **54**, 11169 (1996).
[28] P. E. Blöchl, Phys. Rev. B **50**, 17953 (1994).
[29] G. Kresse and D. Joubert, Phys. Rev. B **59**, 1758 (1999).
[30] J. Perdew and Y. Wang, Phys. Rev. B **45**, 13244 (1992).
[31] Z. Tian, C. S. Tian, D. Sander, and J. Kirschner, Verhandl. DPG **41**, 465 (2006).